sustainability

MDPI

Article

A Circular Economy Approach in the Development of Superabsorbent Polymeric Matrices: Evaluation of the Mineral Retention

Estefanía Álvarez-Castillo [1], Sonia Oliveira [2], Carlos Bengoechea [1,*], Isabel Sousa [2], Anabela Raymundo [2] and Antonio Guerrero [1]

[1] Departamento de Ingeniería Química, Escuela Politécnica Superior, Universidad de Sevilla, C/Virgen de África 7, 41011 Sevilla, Spain; malvarez43@us.es (E.Á.-C.); aguerrero@us.es (A.G.)
[2] LEAF (Linking Landscape, Environment, Agriculture and Food) Research Centre, Instituto Superior de Agronomia, Universidade de Lisboa, Tapada da Ajuda, 1349-017 Lisbon, Portugal; sonia_rocha92@hotmail.com (S.O.); isabelsousa@isa.ulisboa.pt (I.S.); anabraymundo@isa.ulisboa.pt (A.R.)
* Correspondence: cbengoechea@us.es; Tel.: +34-954557179

Abstract: This manuscript focuses on the production of polymeric matrices enriched in minerals and antioxidant compounds. The biopolymers employed are obtained from different by-products of the agro-food industry (porcine plasma protein, pea protein concentrate and soy protein isolate), which helps to revalorize them. Two different manufacturing techniques are employed to produce these matrices: 3D-printing and injection molding. Bioactivity was enhanced through immersion of the samples in magnesium glutamate and iron lactate solutions. To incorporate these minerals and bioactive compounds into the matrices, two additional stages are required: (1) an immersion stage in a mineral/bioactive containing solution, which allows simultaneous removal of the glycerol employed as plasticizer and entrapment of the minerals and bioactive compounds; and (2) a subsequent freeze-drying stage. Matrices produced through these manufacturing processes were assessed through water uptake capacity, mineral analysis, bioactivity and color measurements. The studied matrices have great potential in the food industry, as the threshold for claiming a significant mineral content was reached after the immersion stage. The presence of bioactive compounds could avoid the degradation of these matrices when food processing includes stages at relatively high temperatures.

Keywords: proteins; mineral retention; astaxanthin; antioxidant compounds; 3D-printing; injection molding

Citation: Álvarez-Castillo, E.; Oliveira, S.; Bengoechea, C.; Sousa, I.; Raymundo, A.; Guerrero, A. A Circular Economy Approach in the Development of Superabsorbent Polymeric Matrices: Evaluation of the Mineral Retention. *Sustainability* **2023**, *15*, 12088. https://doi.org/10.3390/su151512088

Academic Editors: Grigorios L. Kyriakopoulos and Marko Vinceković

Received: 6 June 2023
Revised: 24 July 2023
Accepted: 4 August 2023
Published: 7 August 2023

1. Introduction

Three-dimensional printing (3D-printing) is a manufacturing technique that emerged in the 1980s and has impacted several fields in the last decades [1,2]. This is the case in the food industry and in the way meals are being manufactured [3]. Also known as additive manufacturing, 3-D printing is a computer-based production process which deposits a material layer by layer from a cartridge, eventually building up a 3D item [4]. This technique saves and extends raw material customization (sizes and shapes of the product) when compared to subtractive technologies [5,6]. Several materials can be 3D-printed, such as thermoplastics (PLA) [4], glass [7], concrete [8] and even edible materials [9,10]. Thus, this technology has been widely used in the food industry, employing different protein mixtures, such as edible dough, to fill the cartridge [11–13]. The importance of knowledge of the rheological properties of these materials for adequate 3D-printing performance has been highlighted elsewhere [3,10,12]. Although 3D-printing has a huge potential in lots of fields, it could not replace some other manufacturing techniques, which can give modulated properties to the materials, such us excellent reinforcement. In this sense, injection molding is one of the most industrially used manufacturing techniques. It has also been extensively

used to produce biodegradable materials from different protein-based doughs by different researchers [14–16]. This scalable technique requires, just like 3D-printing, a previous mixing of the raw materials. The resulting dough is then pushed into the cavities of the mold, just as dough is pushed out from a reservoir through a nozzle when submitted to a certain pressure [10,17]. In summary, 3D printing is typically recommended for small batch, complex parts, while injection molding is employed mostly for large volume production of less complex parts for which the design stage has already been successfully completed [18]. When comparing manufacturing processes, 3D printing seems to allow an effective use of energy and resources, resulting in a positive environmental impact by reducing waste production and carbon footprint. However, further research into the techno–economic and socio–economic status of 3D printing should be carried out [19].

For this kind of raw material, the use of a plasticizer is required in both techniques, 3D-printed or injection molding, to increase the malleability of the dough during the procedure. The plasticizer used during the study and most commonly employed with protein sources is glycerol [14,16].

The food industry is continuously striving to comply with increasingly demanding safety and quality regulations, as well as to meet customer requirements. The growing awareness of the importance of healthy food is promoting the development of different functional foods which can provide noteworthy benefits to the body's performance. Nutrients (e.g., minerals) are crucial for the proper development of different biological activities in the human body [20]. In this sense, the presence of iron (Fe) in the diet is recommended to avoid anemia, especially in women [21,22]; magnesium (Mg) is involved in more than 600 biochemical reactions and its intake helps in maintaining the muscle and nervous systems, as well as repairing bones [23–25]. Furthermore, the consumption of antioxidants and bioactive compounds also generally improves health. These bioactive compounds, such as astaxanthin pigment [26], may be easily found in some natural marine resources. Astaxanthin is a nutraceutical compound and one of the most powerful antioxidant compounds, extensively used in the food and cosmetics industries [27]. It is extracted from the cell disruption of the *Haematococcus pluvialis*, a green microalga [28]. Thus, the production of food products enriched in these bioactive compounds is an interesting way to introduce them into a healthy diet. When working with these kinds of compounds, controlling the processing parameters is widely important as they can be easily degraded by temperature [29] or storage conditions [30,31], losing or reducing functional properties.

The protein sources used in the production of some of these biodegradable items often come from the food industry as by-products or waste. Th is the case with the porcine plasma protein (PPP) obtained from the surpluses of blood in slaughterhouses [32,33] which is discarded, producing an important environmental issue due to its high organic load. Pea protein concentrate (PPC) is also obtained from the surpluses in pea production [34], and soy protein isolate (SPI) is obtained as a by-product of the soy oil industry [35]. All these protein sources have been extensively studied as raw materials for protein-based products [10,36,37]. The high water absorption capacity of some of these materials [38–40] has already been used by including some specific elements within the protein matrix [41,42]. Furthermore, all three have also been widely used in the food industry as emulsifiers, thickeners or substitutes for another ingredient [43–49].

The main objective of this study is to produce functional snacks through both an emergent and traditional manufacturing technique (3D-printing and injection molding, respectively) in order to obtain edible materials using the protein sources mentioned above (PPP, PPI and SPI) as main raw materials. The high water absorption and swelling ability of the resulting materials is expected to allow the inclusion of different minerals (Mg and Fe) and bioactive compounds (astaxanthin) into the snack when immersed in solutions containing them. The novelty of this work remains in the fact that it will try to take advantage of the high absorbent capacity of these materials to include minerals and bioactive compounds in the matrix. As this is one of the final stages, the bioactive compounds will not be subjected to the high temperatures that are commonly employed in food processing and which degrade their

functional properties. The obtained matrices or snacks were assessed for water absorption capacity, mineral, total phenolic and antioxidant contents.

2. Materials and Methods

2.1. Materials

The main raw materials employed in obtaining the materials developed in the present manuscript were PPP porcine plasma protein (AproPork) from Essentia Proteins (Ankeny, IA, USA); SPI soy protein isolate from SUPRO 500E, Dupont (Kingston, NY, USA); and PPC pea protein concentrate from Pisane® HD, Cosucra (Warcoing, Belgium); the first two were kindly supplied by PROANDA S.A (Sevilla, Spain). Their protein content was determined using a LECO CHNS-932 nitrogen microanalyzer (Leco Corporation, St. Joseph, MI, USA) through % N, which was multiplied by the Kjeldahl factor (6.25). These determinations were made in quadruplicate. The ash content was measured following a protocol already described [16,50], and the Soxhlet method, using hexane as solvent, was carried out to determine the lipids content.

The plasticizer employed during the experimentation, in order to relax the polymeric chains, was Pharma grade glycerol (Gly), which was supplied by Panreac Química S.A (Barcelona, Spain). The salts used in the immersion media were Iron (II) lactate hydrate (from here on, Iron lactate) and Glutamic acid Magnesium salt dehydrate (from here on, Magnesium glutamate), purchased from Sigma Aldrich (St. Louis, MO, USA). Moreover, the astaxanthin used in this study was purchased from Xi'An Natural Field Bio-Technique.

The dough composition was optimized in a previous study, which optimized the composition of analogous systems for their convenient performance in the 3D-printing process [10]. Thus, the selected formulation kept a constant biopolymer/glycerol ratio of 45/55. Within the biopolymer fraction (PPP/PPC/SPI), 1/0/0, 9/1/0 and 8.5/0/1.5 were used.

2.1.1. Mixing of Doughs, 3D-Printing and Injection Molding

In the case of 3D-printed samples, biopolymer/glycerol doughs were obtained, stirring adequate amounts of the ingredients for 10 min at 80 rpm. For this purpose, an IKA-Visc MR-D1 (Staufen, Germany) homogenizer was used at 20 °C with a four-bladed propeller (D: 50 mm) [51]. Afterwards, the homogeneous doughs were 3D-printed into a "duck feet" shape employing a first-generation 3D-printer model from Foodini (Natural Machines, Barcelona, Spain), with a 1.5 mm diameter-nozzle, at 20 °C. This snack shape has been optimized in a previous study to guarantee adequate print details [10]. The printing process took 6.5 min, requiring around 9 mL of dough to print each batch with a flow rate of 0.024 mL/s approximately [10]. On the other hand, doughs with identical composition were injection molded. These doughs were mixed in a two-blade counter-rotating batch mixer Haake Polylab QC (ThermoHaake, Karlsruhe, Germany) at room temperature, at 50 rpm, for 5 min. Afterwards, homogeneous blends were processed into rectangular polymeric probes ($1 \cdot 10 \cdot 60$ mm^3) using a Minijet Piston Injection Molding System (ThermoHaake, Germany). The injection molding parameters used were: 40 and 70 °C for cylinder and mold temperatures, respectively; injection and holding times of 10 and 140 s, respectively; and a pressure of 500 bar for both the injection and holding stage; these parameters were based on previous studies concerning the proteins used in the present manuscript [39].

2.1.2. Preparation of the Salt-Containing and Antioxidant-Containing Solutions

Samples enrichment with Mg and Fe was achieved by immersing the original samples in solutions of magnesium glutamate and iron lactate, during 24 h at room temperature. These salt-containing solutions were prepared using a salt amount equal to 10 and 20 times that required to be considered as a food rich in that certain salt. These claims are specified in the European Regulation No 1169/2011 [52]. According to this regulation, the daily nutrient reference values (NRV) for Fe and Mg in adults are 14 and 375 mg, respectively, and a significant amount of these minerals is considered to be 15% of the NRV per each 100 g. Thus, solutions with a concentration of salts equal to $2.9 \cdot 10^{-3}$ and $5.8 \cdot 10^{-3}$ g/L in

the case of iron lactate and 0.3 and 0.6 g/L in the case of magnesium glutamate were used in this study.

2.2. Methods

2.2.1. Water Uptake Capacity and Soluble Matter Loss

The values of Water Uptake Capacity (WUC) were assessed for all samples, either 3D-printed or injection molded, according to the protocol [17]: polymeric samples were first placed in an oven for 24 h at 50 °C (w_1); then, they were subsequently immersed in deionised water or in a salt-containing solution for 24 h (w_2); and, finally, swollen samples were frozen at −40 °C before being finally dehydrated in a LyoQuest freeze-dryer (Telstar Technologies, Barcelona, Spain) at −80 °C, for 24 h (w_3). Thus, WUC was estimated using Equation (1):

$$WUC\ (\%) = \frac{w_2 - w_3}{w_3} \cdot 100 \quad (1)$$

2.2.2. Mineral Analysis—Induced Coupled Plasma (ICP)

Fe and Mg content were determined in order to know if the snacks produced reached the required standard after their immersion in the salt-containing solutions. Mineral (Mg, Fe) analysis was performed using inductively coupled a plasma (ICP) spectrometry (iCAP Spectrometer equipped with ASX-520 AutoSampler, Thermo Scientific, Waltham, MA, USA). For this purpose, 0.25 g of every lyophilized sample were placed in digestion vessels, where 3 mL of HNO3 and 9 mL of HCl were added to induce the digestion (SCP Science, DigiPREP MS, Baie d'Urfe, QC, Canada). Digestion conditions (1st: 40 °C for 30 min; 2nd: 80 °C for 30 min; and 3rd: 105 °C for 90 min) were carefully controlled throughout the whole process. Afterwards, once the sample cooled down, distilled water was added up to a final volume of 50 mL, and then the solution was allowed to settle down. ICP analysis was carried out for the supernatant [53]. All the samples were measured at least three times.

2.2.3. Color Measurements

The color of samples obtained through the two different processing techniques (3D-printing, injection molding) was modified after being immersed in water or astaxanthin solution. These color changes were assessed employing a CR-400 colorimeter (Minolta, Tokyo, Japan) using illuminant D65 as standard with a visual angle of 2°. The colour variations were studied based on the changes in L^*, a^* and b^* parameters of the CIELAB system, as specified in Equation (2):

$$\Delta E^* = \sqrt{(\Delta a^*)^2 + (\Delta b^*)^2 + (\Delta L^*)^2} \quad (2)$$

2.3. Statistical Analysis

In the present study, all the measurements were performed at least in triplicate and Statgraphics 8 software (The Plains, VA, USA) was used to perform one-way ANOVA tests ($p < 0.05$). Uncertainty was expressed as main values ± standard deviations or by typing superscript letters (lower-case, upper case and Greek) for all the parameters calculated. At least 3 replicates were conducted for any measurement.

3. Results and Discussion

3.1. Characterization of the Protein Sources

The characterization of the protein sources used in the present work gave the results gathered in Table 1, which shows the protein, ashes, moisture and lipids content of the protein sources used. It may be observed that both PPP and PPC were protein concentrates (<90%), while SPI was an isolate (>90%).

Table 1. Basic composition of the protein sources employed during the present study (Porcine Plasma Protein, Soy Protein Isolate and Pea Protein Concentrate).

Composition (%)	PPP	SPI	PPC
Proteins	74.0 ± 1.7	91.8 ± 0.9	88.0 ± 1.2
Ashes	16.0 ± 0.1	5.0 ± 0.2	6.0 ± 0.1
Moisture	9.0 ± 0.4	6.0 ± 0.4	5.0 ± 0.5
Lipids	2.0 ± 0.1	1.0 ± 0.2	1.5 ± 0.2

3.2. Water Uptake Capacity—Effect of the Immersion Media

3.2.1. Water Uptake Capacity in Pure Deionized Water

The water uptake capacity (WUC) values of PPP/PPC/SPI samples (1/0/0, 9/1/0 and 8.5/0/1.5) obtained either through 3D-printing and injection molding (Figure 1A or B, respectively) were tested. When no salt was solubilized, and pure deionized water was used as immersion media (~0% Mg or Fe), no noticeable differences were observed for samples containing PPC or SPI in the formulation (9/1/0 and 8.5/0/1.5, respectively) of 3D-printed samples compared to the corresponding injection moulded samples, in which WUC was always around 2400%. However, the processing technique did affect the WUC values of samples containing only PPP as biopolymer (1/0/0): when these samples were obtained through 3D-printing, lower WUC values were observed (~1800%), when compared to the same formulation processed through injection moulding, with similar WUC values (~2400%) to those of the samples containing SPI or PPC. This can be related to the higher pressure the material suffered during the injection moulding procedure which allows inclusion of more protein in the structure, thus achieving higher sweeling. In any case, all samples showed WUC values that exceeded the superabsorbent threshold (1000%), while keeping their structural integrity for all formulations. These high WUC values highlight the potential of using these samples as a way of incorporating specific ingredients (i.e., bioactive compounds, minerals) through immersion in an aqueous media where they were previously solubilized.

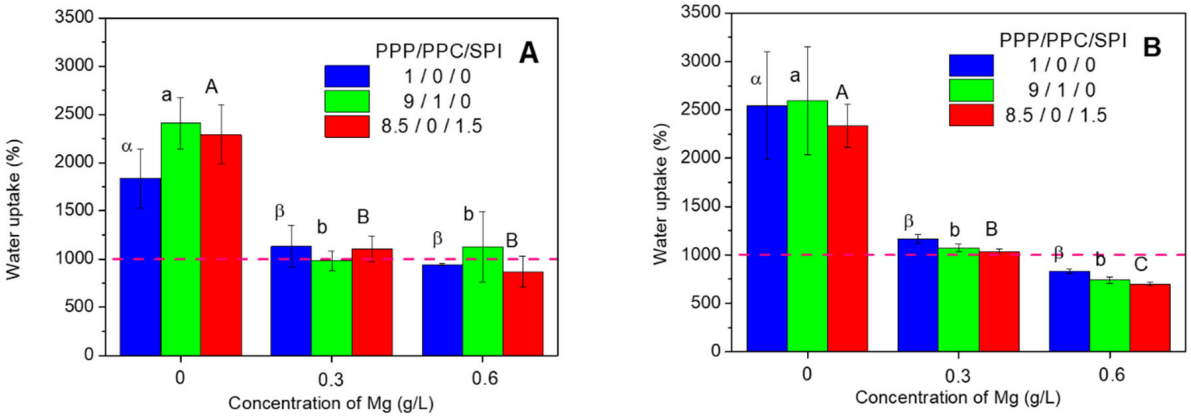

Figure 1. Water uptake capacity of protein-based matrices obtained through 3D-printing (**A**) or injection molding (**B**) after being submitted to immersion in deionized water or magnesium glutamate solutions (0.3 and 0.6 g/L, respectively). The dashed line shows the WUC threshold needed to be considered a superabsorbent material. Lower-case, upper-case and Greek letters indicate significantly different values ($p < 0.05$).

3.2.2. Water Uptake Capacity in Magnesium Glutamate Solution

WUC was then measured by immersing samples in aqueous media with different magnesium glutamate content (0.3, 0.6 g/L). The concentration selected corresponded to 10 and 20 times, respectively, the amount of Mg required for a product to be considered rich in this element. As can be seen from Figure 1, WUC dramatically dropped in the presence of the magnesium salt (by more than a half for all samples when the amount of salt added

was 0.6 mg/L), independently of the processing technique (3D-Printing, injection molding) or the sample composition (PPP/PPC/SPI: 1/0/0, 9/1/0, 8.5/0/1.5). This fact might be related to higher ionic strength in the solution due to the presence of the salts, which is commonly associated with a hindering of the ability of samples to absorb water [54,55]. The decrease in WUC seems to be related to the salt content, especially for injection molding samples, as WUC barely reached the superabsorbent threshold (1000%) when immersed in a 0.3 g/L solution, and then most samples definitely lost their superabsorbent properties when the amount of salt was duplicated (0.6 g/L). The only exception was the 3D-printed 9/1/0 sample containing PPC (Figure 1A), whose WUC values were fairly similar for both salt contents.

3.2.3. Water Uptake Capacity in Iron Lactate Solution

WUC was also measured when samples were immersed in aqueous solutions containing different levels of iron lactate, specifically $2.9 \cdot 10^{-3}$ and $5.8 \cdot 10^{-3}$ g/L, which, respectively, correspond to 10 and 20 times the amount of Fe required for samples to be considered rich in this element. Compared to magnesium glutamate, the addition of iron lactate to the immersion media clearly showed (Figure 2) a much lower impact on WUC, as values were now closer to those obtained for samples immersed in deionised water. In the case of samples prepared exclusively with Gly and PPP (1/0/0), either 3D-printed or injection molded, WUC displayed no significant differences when adding the iron salt to the immersion media. However, samples which also included PPC or SPI (9/1/0, 8.5/0/1.5) displayed a certain decrease in WUC in the presence of iron lactate, although not so drastic as to lose their superabsorbent character, displaying the lowest WUC value observed over 1500%. This lower impact on WUC in the presence of iron lactate compared to magnesium glutamate might be associated with the amount of salt required to reach the claims, as for Fe it is much lower than that required for Mg. Thus, the amount of salt added to the immersion media was around 100 times smaller in the case of iron lactate, due to its lower claim, compared with magnesium glutamate. A lower amount of salt resulted in a lower ionic strength in the immersion media, which permitted water to enter the polymeric network to a greater extent, as a high ionic strength has been reported to inhibit the swelling of superabsorbent gels [54].

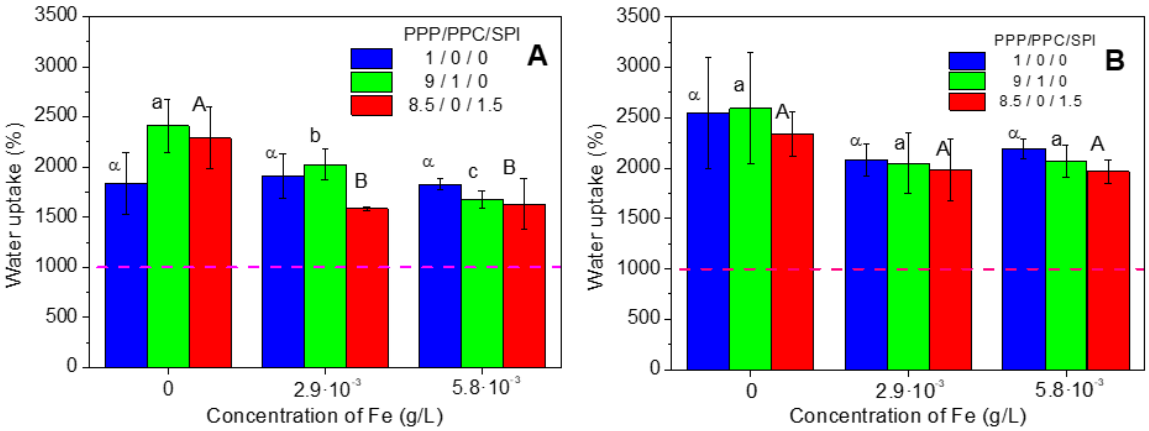

Figure 2. Water uptake capacity of protein-based matrices obtained through 3D-printing (**A**) or injection molding (**B**) after being submitted to immersion in deionized water or iron lactate solutions ($2.9 \cdot 10^{-3}$ and $5.8 \cdot 10^{-3}$ g/L). The dashed line shows the WUC threshold necessary to be considered a superabsorbent material. Lower-case, upper-case and Greek letters indicate significantly different values ($p < 0.05$).

Morphological changes after water immersion were quite apparent, specially for 3D-printed samples, whose shape was more complex than that obtained by injection molding. Thus, higher WUC values resulted in a certain loss of detail in the shape when compared to the original sample before immersion (Appendix A, Figure A1).

3.3. Assessment of the Magnesium and Iron Incorporated into Polymeric Samples

3.3.1. Magnesium

The amount of Mg in every sample (PPP/PPC/SPI: 1/0/0, 9/1/0, and 8.5/0/1.5) immersed in deionized water, as estimated through the ICP technique (Figure 3), was enough to achieve the claim. Neither the 3D-Printed (Figure 3A) nor injection molded samples (Figure 3B) contained enough Mg (at least 562.5 mg/kg of the sample). Figure 3 also shows that none of the studied protein sources possessed an important amount of this mineral before immersion in the magnesium glutamate aqueous solution. However, samples immersed in a magnesium glutamate solution showed a noticeable increase in Mg content (Figure 3). In the case of the amount of magnesium glutamate included in the aqueous solution being 10 times that required to reach the Mg claim (0.3 g/L), all samples reached the claim point for Mg, with the sample that contained plasma and pea protein (9/1/0) showing the lowest value. The highest value, more than 15 times the content required for the claim, was obtained for the sample containing plasma and soy protein (8.5/0/1.5). For samples containing only plasma (1/0/0), the amount of Mg prompted at least four times. When samples were immersed in a solution containing 20 times the amount of Mg required for its claim, a remarkable increase in the amount of Mg present in samples took place, except for the 3D-printed 1/0/0 sample (Figure 3A). This was the only sample that did not contain a higher amount of Mg when immersed in a salt solution of high concentration. Therefore, in general, immersing the samples in a dissolution, which contained Mg salt generally increases the Mg content within the structure, affirming that the mineral was entrapped within the protein structure. Other research included Mg in their samples in order to take advantage of its benefits by itself (also to reduce bitterness [56]) or together with other compounds, such as proteins [57].

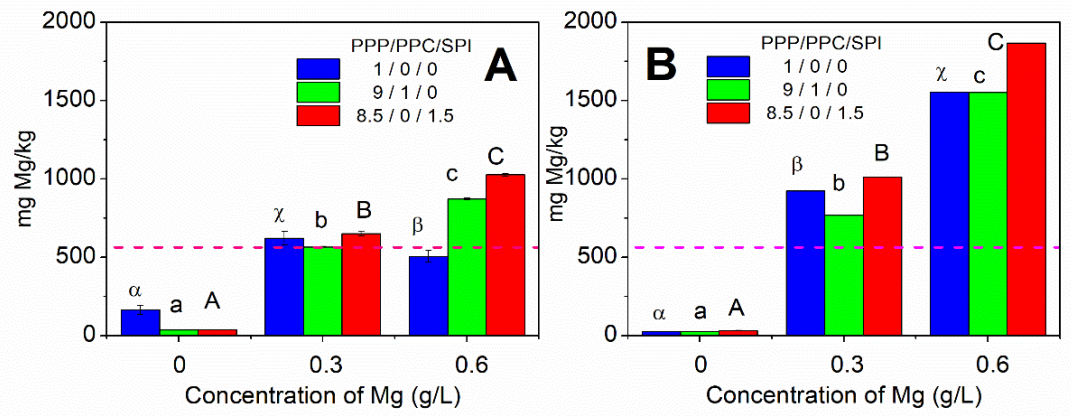

Figure 3. Amount of Mg present in protein-based matrices obtained through 3D-printing (**A**) or injection molding (**B**) after being submitted to immersion in deionized water or magnesium glutamate solutions (0.3 and 0.6 g/L). The dashed line shows the claim required to be considered rich in Mg. Lower-case, upper-case and Greek letters indicate significantly different values ($p < 0.05$).

3.3.2. Iron

When the Fe content of both samples obtained through 3D-printing (Figure 4A) or injection molding (Figure 4B) was determined after immersion in deionized water, the amount of Fe was enough to satisfy the claim of matrices being rich in this mineral (21 mg Fe/kg), as expected, since the PPP source is blood. Only 3D-printed samples containing PPC (9/1/0) possessed a Fe content slightly below the claim. To make these snacks rich enough in iron to be used as functional foods for iron deficiencies, knowing that iron has a problematic absorption, an iron salt was included in the immersion media (Figure 4), and the amount of Fe contained in the sample generally increased. However, 3D-printed samples did not show a clear evolution along with the iron lactate content in the immersion media. Thus, the 8.5/0/1.5 sample was the only one that kept the same iron content when the concentration of iron lactate in the immersion media shifted from 0 to 10 times the claim.

When the iron concentration in the immersion media was 20 times the claim, a decrease in the iron content, after immersion in the less concentrated solution, was detected, which is similar to the evolution previously commented on for the 3D-printed 1/0/0 sample. This might be linked to the high quantity of salt in the immersion media, which hinders the entrapment of water within the sample, inhibiting its swelling. The resulting smaller pores would hardly retain the salt after freeze-drying. On the other hand, injection molded samples always showed an increasing trend in iron content when immersed in solutions with a higher iron lactate concentration. For example, the iron content for the 1/0/0 sample was duplicated and triplicated after immersion in $2.9{\cdot}10^{-3}$ and $5.8{\cdot}10^{-3}$ g/L solutions, respectively, as PPP matrix, being from blood, reflects a high affinity with Iron. Thus, immersion in the iron salt solution, seems to be an appropriate technique to satisfactorily include iron within the protein-based samples. Thus, other studies have also dealt with the incorporation of Fe into the food item, such as bread [57,58] or emulsions [59], but by adding the salt that contains the mineral directly to the raw materials.

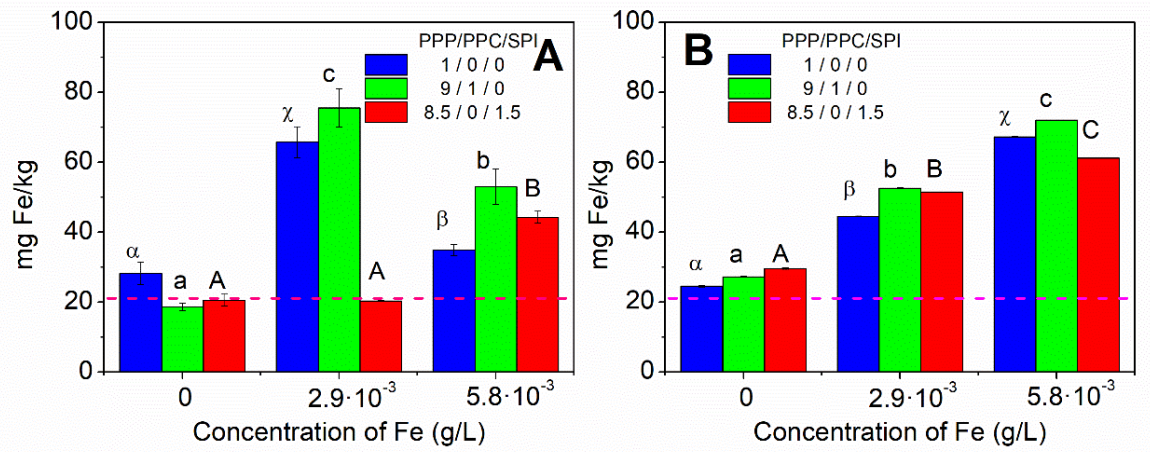

Figure 4. Amount of Fe present in protein-based matrices through 3D-printing (**A**) or injection molding (**B**) after being submitted to immersion in deionized water or iron lactate ($2.9{\cdot}10^{-3}$ and $5.8{\cdot}10^{-3}$ g/L). The dashed line shows the claim to be considered rich in Fe. Lower-case, upper-case and Greek letters indicate significantly different values ($p < 0.05$).

3.4. Color Measurements

Color is an essential quality parameter in the food industry as it is the first visual attribute evaluated by consumers. Table 2 gathers the color parameters obtained through CIELAB systems to quantify the color differences among the different samples. The parameter L*, representing the lightness of the samples, decreased for all samples that were immersed in astaxanthin solution, except for injection molded samples containing only plasma as protein source (1/0/0), which presented a slight increase in lightness. The parameter a* specifies the chromatic differences from greenness (negative value) to redness (positive value). All samples immersed in astaxanthin solution showed higher values of a* than those immersed in deionized water. This fact was associated with the orange/red colour of astaxanthin [60], which can be used as a natural pigment [61]. The parameter b* makes reference to the blueness (negative value) and to the yellowness (positive value). Only the 3D-printed samples obtained from PPP and SPI increased the values of b* (Δb*), gaining a yellow color, when they were immersed in astaxanthin solution. The rest of the samples reduced or approximately kept the same b* values. The ΔE* values indicate total colour differences, which must be above 5 to be perceived by the human eye [62]. Thus, only 3D-printed matrices obtained from PPP and SPI experienced a perceptible change in color when immersed in the astaxanthin solution.

Table 2. Color parameters of 3D-printed or injection molded protein-based matrices after being submitted to immersion in deionized water or astaxanthin solution. Lower, upper-case and Greek letters indicate significantly different values ($p < 0.05$).

		L*	a*	b*	ΔE*
3D-Printing	1/0/0	79.04 ^{g}	4.75 ^{C}	24.01 $^{\gamma}$	
	1/0/0 ast	74.46 ^{d,e}	6.89 ^{F}	24.75 $^{\delta}$	5.12
	8.5/0/1.5	81.98 ^{h}	3.66 ^{B}	21.86 $^{\gamma}$	
	8.5/0/1.5 ast	78.26 ^{f,g}	6.02 ^{D,E}	25.52 $^{\varepsilon}$	5.73
	9/1/0	81.23 ^{h}	3.07 ^{A}	22.12 $^{\alpha}$	
	9/1/0 ast	77.88 ^{f}	6.30 ^{E}	23.37 $^{\beta}$	4.82
Injection-moulding	1/0/0	71.33 ^{a}	6.95 ^{F}	31.41 $^{\theta}$	
	1/0/0 ast	73.08 ^{b,c}	8.10 ^{G}	28.30 $^{\eta}$	4.05
	8.5/0/1.5	73.74 ^{c,d}	6.00 ^{D,E}	28.30 $^{\eta}$	
	8.5/0/1.5 ast	72.85 ^{b}	7.78 ^{G}	27.69 $^{\zeta}$	2.08
	9/1/0	74.96 ^{e}	5.515 ^{D}	28.21 $^{\zeta,\eta}$	
	9/1/0 ast	72.99 ^{e}	7.99 ^{D}	28.26 $^{\eta}$	3.16

The fact that these samples can incorporate astaxanthin is promising, as they could be potentially used in the development of bioactive snacks. However, further research is required to assure compliance with current regulations.

4. Concluding Remarks

Matrices from different protein resources (porcine plasma protein, pea protein concentrate and soy protein isolate) can be obtained through two different manufacturing strategies, 3D-printing and injection moulding. Moreover, the water absorption of these hydrophilic protein snacks could be employed to include minerals, such as magnesium or iron, and/or different beneficial compounds, such as astaxanthine, in the formulation.

Samples were immersed in aqueous solutions that included the desired ingredient (magnesium glutamate, iron lactate or astaxanthine), incorporated into the protein snack during the absorption process. Even if water absorption capacity dramatically decreased in the aqueous solution of the salts selected, especially at higher salt contents, all samples immersed in these solutions achieve the amount of Mg or Fe required to satisfy the claim. This is specially important in the case of Mg, as original samples were below the content required to reach the claim, while samples already reached the Fe claim before immersion in iron lactate solution. Protein matrices or snacks with superabsorbent properties could be obtained, independently as to whether they are obtained through 3D printing or injection molding, typically showing greater mineral content after the immersion stage at higher salt contents. It should be highlighted that the freeze-drying step used at laboratory scale in the present work should be replaced at industrial scale by cheaper, and more energy efficient alternatives.

Author Contributions: Conceptualization, E.Á.-C. and A.R.; validation, A.R., I.S., C.B. and A.G.; formal analysis, E.Á.-C. and S.O.; investigation, E.Á.-C. and S.O.; resources, A.R., C.B. and A.G.; data curation, E.Á.-C. and S.O.; writing—original draft preparation, E.Á.-C.; writing—review and editing, C.B., A.R., I.S. and A.G.; supervision, A.R. and C.B.; project administration, C.B., A.R. and A.G.; funding acquisition, A.R., I.S., C.B. and A.G. Furthermore, all authors have read and agreed to this version of the study. All authors have read and agreed to the published version of the manuscript.

Funding: This study was financially supported by the Portuguese Fundação para a Ciência e Tecnologia (FCT) through the research unit LEAF—Linking Landscape, Environment, Agriculture and Food UID/AGR/04129/2020. Additionally, this research was part of the project PID2021-124294OB-C21 funded by MCIN/AEI/10.13039/501100011033/ and by "ERDF A way of making Europe".

Institutional Review Board Statement: Not applicable.

Informed Consent Statement: Not applicable.

Data Availability Statement: All the results showed in the manuscript could be requested to the corresponding author who would provide them.

Acknowledgments: This work was funded by the Portuguese Fundação para a Ciência e Tecnologia (FCT) through the research unit LEAF—Linking Landscape, Environment, Agriculture and Food UID/AGR/04129/2020 and the Spanish "Ministerio de Ciencia e Innovación (MCI)/Agencia Estatal de Investigación (AEI)/Fondo Europeo de Desarrollo Regional (FEDER, UE)" for the financial support provided through the funding of the PID2021–124294OB-C21 (MCI/AEI/FEDER, UE) project. The authors would also thank Spanish Ministerio de Universidades for the PhD grant: PRE2019-089815 awarded to E. Álvarez-Castillo.

Conflicts of Interest: All the authors confirm that the manuscript has not been previously published, being an original work. The authors also declare that they have no known competing financial interest or personal relationship that could have appeared to influence the work reported in this paper.

Appendix A

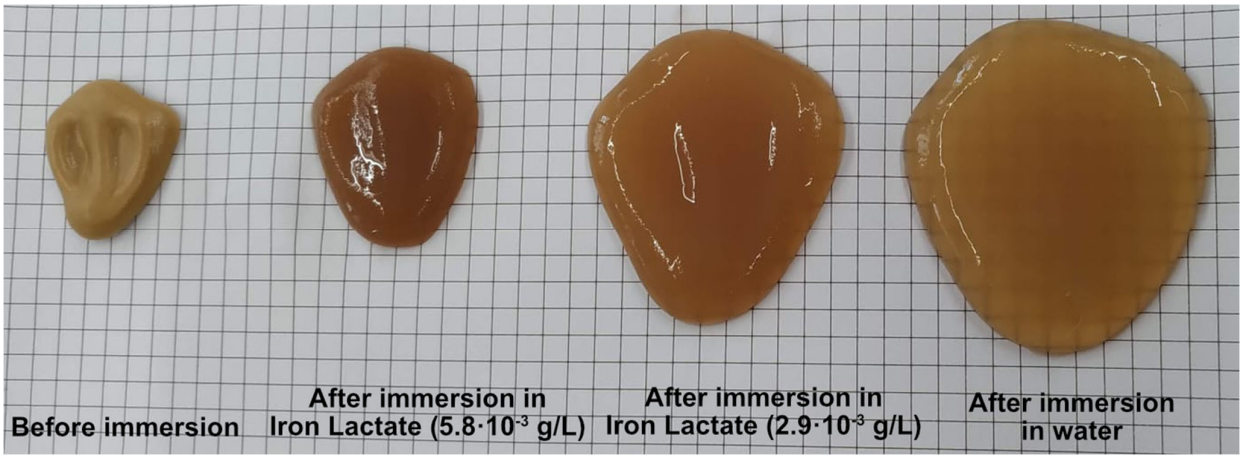

Figure A1. Images of PPP/PPC/SPI (1/0/0) printed samples before and after immersion in iron lactate solutions (0, $2.9{\cdot}10^{-3}$ and $5.8{\cdot}10^{-3}$ g/L).

References

1. Saptarshi, S.M.; Zhou, D.C. *Basics of 3D Printing*; Elsevier Inc.: Amsterdam, The Netherlands, 2019; ISBN 9780323581189.
2. Dankar, I.; Haddarah, A.; Omar, F.E.L.; Sepulcre, F.; Pujolà, M. 3D printing technology: The new era for food customization and elaboration. *Trends Food Sci. Technol.* **2018**, *75*, 231–242. [CrossRef]
3. Nijdam, J.J.; Agarwal, D.; Schon, B.S. Assessment of a novel window of dimensional stability for screening food inks for 3D printing. *J. Food Eng.* **2021**, *292*, 110349. [CrossRef]
4. Serra, T.; Planell, J.A.; Navarro, M. High-resolution PLA-based composite scaffolds via 3-D printing technology. *Acta Biomater.* **2013**, *9*, 5521–5530. [CrossRef]
5. Li, N.; Qiao, D.; Zhao, S.; Lin, Q.; Zhang, B.; Xie, F. 3D printing to innovate biopolymer materials for demanding applications: A review. *Mater. Today Chem.* **2021**, *20*, 100459. [CrossRef]
6. Sun, J.; Zhou, W.; Huang, D.; Fuh, J.Y.H.; Hong, G.S. An Overview of 3D Printing Technologies for Food Fabrication. *Food Bioprocess Technol.* **2015**, *8*, 1605–1615. [CrossRef]
7. Wu, W.; Du, H.; Sui, H.; Sun, B.; Wang, B.; Yu, Z.; Ni, H.; Li, G.; Zhao, J. Study of printing parameters of pneumatic-injection 3D printing of Fe-based metallic glass. *J. Non-Cryst. Solids* **2018**, *489*, 50–56. [CrossRef]
8. Vantyghem, G.; De Corte, W.; Shakour, E.; Amir, O. 3D printing of a post-tensioned concrete girder designed by topology optimization. *Autom. Constr.* **2020**, *112*, 103084. [CrossRef]
9. Derossi, A.; Caporizzi, R.; Oral, M.O.; Severini, C. Analyzing the effects of 3D printing process per se on the microstructure and mechanical properties of cereal food products. *Innov. Food Sci. Emerg. Technol.* **2020**, *66*, 102531. [CrossRef]
10. Álvarez-Castillo, E.; Oliveira, S.S.; Bengoechea, C.; Sousa, I.; Raymundo, A.; Guerrero, A. A rheological approach to 3D printing of plasma protein based doughs. *J. Food Eng.* **2020**, *288*, 110255. [CrossRef]
11. Gao, J.; Liu, J.; Peng, H.; Wang, Y.; Cheng, S.; Lei, Z. Preparation of a low-cost and eco-friendly superabsorbent composite based on wheat bran and laterite for potential application in Chinese herbal medicine growth. *R. Soc. Open Sci.* **2018**, *5*, 180007. [CrossRef]

12. Xu, L.; Gu, L.; Su, Y.; Chang, C.; Wang, J.; Dong, S.; Liu, Y.; Yang, Y.; Li, J. Impact of thermal treatment on the rheological, microstructural, protein structures and extrusion 3D printing characteristics of egg yolk. *Food Hydrocoll.* **2020**, *100*, 105399. [CrossRef]
13. Rahman, J.M.H.; Shiblee, M.D.N.I.; Ahmed, K.; Khosla, A.; Kawakami, M.; Furukawa, H. Rheological and mechanical properties of edible gel materials for 3D food printing technology. *Heliyon* **2020**, *6*, e05859. [CrossRef] [PubMed]
14. Fernández-Espada, L.; Bengoechea, C.; Cordobés, F.; Guerrero, A. Thermomechanical properties and water uptake capacity of soy protein-based bioplastics processed by injection molding. *J. Appl. Polym. Sci.* **2016**, *133*, 43524. [CrossRef]
15. Álvarez-Castillo, E.; Bengoechea, C.; Guerrero, A. Composites from by-products of the food industry for the development of superabsorbent biomaterials. *Food Bioprod. Process.* **2020**, *119*, 296–305. [CrossRef]
16. Perez-Puyana, V.; Felix, M.; Romero, A.; Guerrero, A. Characterization of pea protein-based bioplastics processed by injection moulding. *Food Bioprod. Process.* **2016**, *97*, 100–108. [CrossRef]
17. Álvarez-Castillo, E.; Bengoechea, C.; Rodríguez, N.; Guerrero, A. Development of green superabsorbent materials from a by-product of the meat industry. *J. Clean. Prod.* **2019**, *223*, 651–661. [CrossRef]
18. Boros, R.; Kannan Rajamani, P.; Kovacs, J.G. Combination of 3D printing and injection molding: Overmolding and overprinting. *Express Polym. Lett.* **2019**, *13*, 889–897. [CrossRef]
19. Yoha, K.S.; Moses, J.A. 3D Printing Approach to Valorization of Agri-Food Processing Waste Streams. *Foods* **2023**, *12*, 212. [CrossRef]
20. Costa, G.T.; Vasconcelos, Q.D.J.S.; Abreu, G.C.; Albuquerque, A.O.; Vilar, J.L.; Aragão, G.F. Systematic review of the ingestion of fructooligosaccharides on the absorption of minerals and trace elements versus control groups. *Clin. Nutr. ESPEN* **2021**, *41*, 68–76. [CrossRef]
21. Abu-Baker, N.N.; Eyadat, A.M.; Khamaiseh, A.M. The impact of nutrition education on knowledge, attitude, and practice regarding iron deficiency anemia among female adolescent students in Jordan. *Heliyon* **2021**, *7*, e06348. [CrossRef]
22. Mohan, A.; Manikandanesan, S.; Manickam, P.; Kolandaswamy, K.; Murhekar, M. Informing primi and elderly pregnant women about iron sucrose administration for moderate anemia can improve treatment compliance in public health facilities, Kancheepuram health district, Tamil Nadu, India, 2017: A cross-sectional study. *Clin. Epidemiol. Glob. Health* **2021**, *10*, 100681. [CrossRef]
23. Pardo, M.R.; Vilar, E.G.; Martín, I.S.M.; Martín, M.A.C. Bioavailability of magnesium food supplements: A systematic review. *Nutrition* **2021**, *89*, 111294. [CrossRef] [PubMed]
24. Zhou, H.; Liang, B.; Jiang, H.; Deng, Z.; Yu, K. Magnesium-based biomaterials as emerging agents for bone repair and regeneration: From mechanism to application. *J. Magnes. Alloys* **2021**, *9*, 779–804. [CrossRef]
25. Porri, D.; Biesalski, H.K.; Limitone, A.; Bertuzzo, L.; Cena, H. Effect of magnesium supplementation on women's health and well-being. *NFS J.* **2021**, *23*, 30–36. [CrossRef]
26. Chandra Roy, V.; Ho, T.C.; Lee, H.-J.; Park, J.-S.; Nam, S.Y.; Lee, H.; Getachew, A.T.; Chun, B.-S. Extraction of astaxanthin using ultrasound-assisted natural deep eutectic solvents from shrimp wastes and its application in bioactive films. *J. Clean. Prod.* **2021**, *284*, 125417. [CrossRef]
27. Ren, Y.; Deng, J.; Huang, J.; Wu, Z.; Yi, L.; Bi, Y.; Chen, F. Using green alga *Haematococcus pluvialis* for astaxanthin and lipid co-production: Advances and outlook. *Bioresour. Technol.* **2021**, *340*, 125736. [CrossRef] [PubMed]
28. Kim, B.; Youn Lee, S.; Lakshmi Narasimhan, A.; Kim, S.; Oh, Y.-K. Cell disruption and astaxanthin extraction from *Haematococcus pluvialis*: Recent advances. *Bioresour. Technol.* **2022**, *343*, 126124. [CrossRef]
29. Özşen, D.; Erge, H.S. Degradation Kinetics of Bioactive Compounds and Change in the Antioxidant Activity of Wild Strawberry (*Fragaria vesca*) Pulp During Heating. *Food Bioprocess Technol.* **2013**, *6*, 2261–2267. [CrossRef]
30. Duru, N.; Karadeniz, F.; Erge, H.S. Changes in Bioactive Compounds, Antioxidant Activity and HMF Formation in Rosehip Nectars During Storage. *Food Bioprocess Technol.* **2012**, *5*, 2899–2907. [CrossRef]
31. Patras, A.; Brunton, N.P.; Tiwari, B.K.; Butler, F. Stability and Degradation Kinetics of Bioactive Compounds and Colour in Strawberry Jam during Storage. *Food Bioprocess Technol.* **2011**, *4*, 1245–1252. [CrossRef]
32. Sanders, B. Global Pig Slaughter Statistics and Charts. 2018. Available online: https://faunalytics.org/global-pig-slaughter-statistics-and-charts/ (accessed on 5 June 2023).
33. Gatnau, R.; Polo, J.; Robert, E. Plasma protein antimicrobialsubstitution at negligible risk. In *Feed Manufacturing in the Mediterranean Region. Improving Safety: From Feed to Food*; Brufau, J., Ed.; CIHEAM-IAMZ: Zaragoza, Spain, 2001; pp. 141–150.
34. Tulbek, M.C.; Lam, R.S.H.; Wang, Y.C.; Asavajaru, P.; Lam, A. Chapter 9—Pea: A Sustainable Vegetable Protein Crop. In *Sustainable Protein Sources*; Nadathur, S.R., Wanasundara, J.P.D., Scanlin, L., Eds.; Academic Press: San Diego, CA, USA, 2017; pp. 145–164. ISBN 978-0-12-802778-3.
35. Tian, H.; Guo, G.; Xiang, A.; Zhong, W.H. Intermolecular interactions and microstructure of glycerol-plasticized soy protein materials at molecular and nanometer levels. *Polym. Test.* **2018**, *67*, 197–204. [CrossRef]
36. Cho, S.Y.; Rhee, C. Mechanical properties and water vapor permeability of edible films made from fractionated soy proteins with ultrafiltration. *LWT—Food Sci. Technol.* **2004**, *37*, 833–839. [CrossRef]
37. Fernández-Espada, L.; Bengoechea, C.; Cordobés, F.; Guerrero, A. Protein/glycerol blends and injection-molded bioplastic matrices: Soybean versus egg albumen. *J. Appl. Polym. Sci.* **2016**, *133*, 42980. [CrossRef]

38. Cuadri, A.A.A.; Romero, A.; Bengoechea, C.; Guerrero, A. Natural superabsorbent plastic materials based on a functionalized soy protein. *Polym. Test.* **2017**, *58*, 126–134. [CrossRef]
39. Álvarez-Castillo, E.; Pelagio, M.J.; Bengoechea, C.; Guerrero, A. Plasma based superabsorbent materials modulated through chemical cross-linking. *J. Environ. Chem. Eng.* **2021**, *9*, 105017. [CrossRef]
40. Álvarez-Castillo, E.; Del Toro, A.; Aguilar, J.M.; Guerrero, A.; Bengoechea, C. Optimization of a thermal process for the production of superabsorbent materials based on a soy protein isolate. *Ind. Crops Prod.* **2018**, *125*, 573–581. [CrossRef]
41. Jiménez-Rosado, M.; Pérez-Puyana, V.; Cordobés, F.; Romero, A.; Guerrero, A. Development of soy protein-based matrices containing zinc as micronutrient for horticulture. *Ind. Crops Prod.* **2018**, *121*, 345–351. [CrossRef]
42. Jiménez-Rosado, M.; Perez-Puyana, V.; Sánchez-Cid, P.; Guerrero, A.; Romero, A. Incorporation of ZnO Nanoparticles into Soy Protein-Based Bioplastics to Improve Their Functional Properties. *Polymers* **2021**, *13*, 486. [CrossRef]
43. Glusac, J.; Davidesko-Vardi, I.; Isaschar-Ovdat, S.; Kukavica, B.; Fishman, A. Tyrosinase-crosslinked pea protein emulsions: Impact of zein incorporation. *Food Res. Int.* **2019**, *116*, 370–378. [CrossRef] [PubMed]
44. Hurtado, S.; Saguer, E.; Toldrà, M.; Parés, D.; Carretero, C. Porcine plasma as polyphosphate and caseinate replacer in frankfurters. *Meat Sci.* **2012**, *90*, 624–628. [CrossRef]
45. Hurtado, S.; Dagà, I.; Espigulé, E.; Parés, D.; Saguer, E.; Toldrà, M.; Carretero, C. Use of porcine blood plasma in "phosphate-free frankfurters". *Procedia Food Sci.* **2011**, *1*, 477–482. [CrossRef]
46. Nakauma, M.; Funami, T.; Noda, S.; Ishihara, S.; Al-Assaf, S.; Nishinari, K.; Phillips, G.O. Comparison of sugar beet pectin, soybean soluble polysaccharide, and gum arabic as food emulsifiers. 1. Effect of concentration, pH, and salts on the emulsifying properties. *Food Hydrocoll.* **2008**, *22*, 1254–1267. [CrossRef]
47. Raeker, M.Ö.; Johnson, L.A. Thermal and Functional Properties of Bovine Blood Plasma and Egg White Proteins. *J. Food Sci.* **1995**, *60*, 685–690. [CrossRef]
48. Sridharan, S.; Meinders, M.B.J.; Bitter, J.H.; Nikiforidis, C. V Pea flour as stabilizer of oil-in-water emulsions: Protein purification unnecessary. *Food Hydrocoll.* **2020**, *101*, 105533. [CrossRef]
49. Zhang, S.; Holmes, M.; Ettelaie, R.; Sarkar, A. Pea protein microgel particles as Pickering stabilisers of oil-in-water emulsions: Responsiveness to pH and ionic strength. *Food Hydrocoll.* **2020**, *102*, 105583. [CrossRef]
50. Horwitz, W.; Chichilo, P.; Reynolds, H. *Official Methods of Analysis of the Association of Official Analytical Chemists*; Association of Official Analytical Chemists: Washington, DC, USA, 1970.
51. Demirkesen, I. Formulation of Chestnut Cookies and their Rheological and Quality Characteristics. *J. Food Qual.* **2016**, *39*, 264–273. [CrossRef]
52. The European Parliament and the Council of the European Union. Regulation (EU) 1169/2011 on the provision of food information to consumers, amending Regulations (EC) No 1924/2006 and (EC) No 1925/2006 of the European Parliament and of the Council, and repealing Commission Directive 87/250/EEC, Council Directive 90/49. *Off. J. Eur. Union* **2011**, *17*, 18–63.
53. Fradinho, P.; Raymundo, A.; Sousa, I.; Domínguez, H.; Torres, M.D. Edible Brown Seaweed in Gluten-Free Pasta: Technological and Nutritional Evaluation. *Foods* **2019**, *8*, 622. [CrossRef]
54. Bao, Y.; Ma, J.; Li, N. Synthesis and swelling behaviors of sodium carboxymethyl cellulose-g-poly(AA-co-AM-co-AMPS)/MMT superabsorbent hydrogel. *Carbohydr. Polym.* **2011**, *84*, 76–82. [CrossRef]
55. Álvarez-Castillo, E.; Aguilar, J.M.; Bengoechea, C.; López-Castejón, M.L.; Guerrero, A. Rheology and Water Absorption Properties of Alginate–Soy Protein Composites. *Polymers* **2021**, *13*, 1807. [CrossRef] [PubMed]
56. Sun-Waterhouse, D.; Wadhwa, S.S. Industry-Relevant Approaches for Minimising the Bitterness of Bioactive Compounds in Functional Foods: A Review. *Food Bioprocess Technol.* **2013**, *6*, 607–627. [CrossRef]
57. Kabakci, C.; Sumnu, G.; Sahin, S.; Oztop, M.H. Encapsulation of Magnesium with Lentil Flour by Using Double Emulsion to Produce Magnesium Enriched Cakes. *Food Bioprocess Technol.* **2021**, *14*, 1773–1790. [CrossRef]
58. Kiskini, A.; Kapsokefalou, M.; Yanniotis, S.; Mandala, I. Effect of Iron Fortification on Physical and Sensory Quality of Gluten-Free Bread. *Food Bioprocess Technol.* **2012**, *5*, 385–390. [CrossRef]
59. Saffarionpour, S.; Diosady, L.L. Multiple Emulsions for Enhanced Delivery of Vitamins and Iron Micronutrients and Their Application for Food Fortification. *Food Bioprocess Technol.* **2021**, *14*, 587–625. [CrossRef]
60. Tume, R.K.; Sikes, A.L.; Tabrett, S.; Smith, D.M. Effect of background colour on the distribution of astaxanthin in black tiger prawn (*Penaeus monodon*): Effective method for improvement of cooked colour. *Aquaculture* **2009**, *296*, 129–135. [CrossRef]
61. Batista, A.P.; Nunes, M.C.; Fradinho, P.; Gouveia, L.; Sousa, I.; Raymundo, A.; Franco, J.M. Novel foods with microalgal ingredients—Effect of gel setting conditions on the linear viscoelasticity of Spirulina and *Haematococcus* gels. *J. Food Eng.* **2012**, *110*, 182–189. [CrossRef]
62. Castellar, M.R.; Obón, J.M.; Fernández-López, J.A. The isolation and properties of a concentrated red-purple betacyanin food colourant from *Opuntia stricta* fruits. *J. Sci. Food Agric.* **2006**, *86*, 122–128. [CrossRef]